ORIGINAL ARTICLE

Vertical dust concentration measurements within the boundary layer to assess regional source–sink relations of dust in semi-arid grasslands of Inner Mongolia, China

Matthias Reiche · Roger Funk · Carsten Hoffmann · Zhuodong Zhang · Michael Sommer

Abstract Whether grazed semi-arid grassland can be regarded as a net-sink or net-source of aeolian dust is difficult to detect since deposition and emission processes are in gradual transition. In grassland, dust arrives from sources far away or is directly emitted and immediately part of the suspension load. The processes of dust emission or deposition can be mainly identified by vertical concentration measurements close to the ground and close to the sources. Often the concentration differences at the used measuring heights are too small to derive the direction of vertical fluxes precisely, especially at dust storms of light-to-medium intensities. For this reason, particle mass (PM_{10}, PM_1) and particle number concentrations were measured simultaneously at ground level and at heights of up to 80 m using a dust monitoring system lifted by a kite. The measured data of dust concentration gradients are used to calculate the vertical fluxes with the necessary certainty to derive the direction of the dust fluxes. Additionally, dust arriving from different directions and crossing different land use/land cover patterns was used to interpret the interaction of source/sink relationships along the transport direction upstream of the measuring point. Results show that dust measurements above grassland have to span greater height differences to derive vertical fluxes certainly, i.e., concentration gradients ($\Delta c/\Delta z$) of PM_{10} and PM_1 provide an indication of the direction of the dust flux. Furthermore, the results indicate a close relationship between the particle size compositions of the dust and land use/cover patterns. Arable land in the surroundings causes an emission flux (vertical upward), especially of the coarser fractions >8 μm, whereas grassland causes deposition fluxes of size classes >2 μm during a dust storm of low intensity. Sources from far away are reflected by higher concentrations of finer particles, measured during a super-regional dust storm. Both, dust concentration gradients and particle size composition reflect the potential source areas and deposition processes adequately with regard to different land use/cover patterns up to 50 km away.

Keywords Particulate matter · Vertical dust flux · Kite · Kite-borne investigation · PM mass-size composition

M. Reiche (✉) · R. Funk · C. Hoffmann · M. Sommer
Institute of Soil Landscape Research, Leibniz-Centre for Agricultural Landscape Research (ZALF), Eberswalder Str. 84, 15374 Müncheberg, Germany
e-mail: Matthias.Reiche@zalf.de

Z. Zhang
State Key Laboratory of Earth Surface Processes and Resource Ecology, School of Geography, Beijing Normal University, Beijing 100875, China

M. Sommer
Institute of Earth and Environmental Science, University of Potsdam, Potsdam, Germany

Introduction

Wind-induced dust emissions from arid and semi-arid soils represent the largest primary dust sources (Herman et al. 1997; Prospero et al. 2002), accounting for more than 50 % of the total aerosol amount in the global atmosphere (Andreae 1995; Zender et al. 2004). Emitted particles with diameters less than 20 μm can remain in the atmosphere for a long period of time (Alfaro 2008) and can be transported over thousands of kilometers from the source (Lee et al. 2003; Zhao et al. 2006). Fine dust particles, for example sizes a fraction of $PM_{2.5}$, influence atmospheric processes such as radiation balance or cloud formation and

are relevant in climate change impact processes and air quality problems (IPCC 2013).

Besides the major dust source regions of northern Africa (Sahara) or Asia (Taklimakan, Gobi), vast regions of semi-arid grasslands are affected by wind erosion and have become more relevant in the global dust cycle (Tanaka and Chiba 2006; Shinoda et al. 2010; 2011). In the semi-arid grasslands of Inner Mongolia, which have been a natural sink for dust from sources far away for centuries, a reduction in the grass cover has taken place, caused mainly by a strong increase of grazing intensity (Li et al. 2000). Livestock numbers increased excessively during the last half century from about 8.4 million to more than 71 million in 2003 (Angerer et al. 2008). Livestock grazing reduces soil organic carbon and nitrogen in the top soils (Wen et al. 2013) and make the affected sites more susceptible to wind erosion. In the last decade, the grazing intensity remained constantly at a high level of about 4–5 sheep units per hectare (one sheep unit: refers to one ewe with one lamb) (Butterbach-Bahl et al. 2011), but was compensated by an increased precipitation rate which improved the vegetation cover in this region. Hoffmann et al. (2008a, b) and Funk et al. (2012) derived dust deposition rates depending on the current status of vegetation conditions. They characterized the Xilingol steppe mainly as a dust deposition area due to its moderate grazing intensity.

Desert regions are obvious dust sources, but data is scare on which regions alternately act as dust sources or sinks, such as temperate grasslands. Field measurements are necessary for a better understanding of wind erosion, dust release and deposition processes in these regions. Methods to measure wind erosion processes in steppe regions do not differ from those for agricultural land (Funk et al. 2013), but there are differences which need to be considered if much larger areas are affected, the longer time scales of erosion and/or deposition (Lawrence and Neff 2009), the topography (Goossens 2006; Hoffmann et al. 2008a) and the heterogeneity of vegetation (Tegen et al. 2002; Hoffmann et al. 2008a). Wind erosion and dust emission are mainly measured near ground by towers ≤10 m (Zobeck et al. 2003) because 80–95 % of the material is transported in saltation mode below 1 m height. Dust traps are installed directly at or close to the emission site (Sterk and Raats 1996; Goossens and Offer 2000; Sterk et al. 2004). If the eroded material is transported over long distances and contains a large proportion of dust, the particles are mixed up to greater heights. In order to measure differences in the transported quantities of dust which allow a derivation of vertical fluxes, measuring heights have to be higher. Dong et al. (2010) used a 50 m tower in the Minqin area of China for monitoring PM size concentration and dust flux with modified Big Spring Number Eight (BSNE, Fryrear 1986) samplers.

Recent technical developments in dust measurement devices resulted in small and lightweight dust monitors, which can be lifted up by kite at sufficient wind velocities (Reiche et al. 2012a). Also, new technologies and forms of kites allow its application at a wide range of wind velocities and in a multitude of scientific fields (Balsley et al. 1998; Reiche et al. 2012a). However, in wind erosion studies the use of kites is rare. One study by McTanish et al. (2005) used a kite during a regional dust storm event in Australia to carry a device for PM_{10} measurements. The result of the vertical dust profile was used to calibrate a corresponding satellite image by quantifying a dust cloud (McGowan and Clark 2008).

Vertical dust profiles in semi-arid grassland and the distinction between upward- and downward fluxes are more difficult to determine since the dust concentration is quite uniform near ground level (Hoffmann et al. 2008a). To identify a region as sink or source for aeolian dust, and to separate local from supra-regional dust sources, a clear determination of upward- and downward dust fluxes is necessary. Dust concentration measurements with a compact environmental dust monitor (EDM) lifted by a kite were described by Reiche et al. (2012a). In the study, the applicability of the kite-borne method was proven and uncertainties were discussed. Since dust storms are mainly associated with high wind velocities, kites are advantageous tools compared to balloons or light aircrafts.

The objectives of this study are:

1. To measure horizontal fluxes of particle mass and particle number concentrations at different height levels of several decametres over grassland;
2. To compare particle mass and particle number concentrations at different height levels with the ground station;
3. To determine the vertical dust fluxes;
4. To identify dust deposition or emission processes (source/sink patterns) in grasslands in relation to the land use/cover patterns.

Materials and methods

Study area

The measurements were carried out in the semi-arid grassland of the Xilingol steppe north of the Dalai Nur Lake (43°24′N, 116°38′E) located 90 km southeast of the city of Xilinhot (Fig. 1). The grassland represents a typical steppe ecosystem and is dominated by species of *Leymus chinensis* and *Stipa grandis* (Chen et al. 2005). The climate is characterized by semi-arid conditions with cold and dry winters and warm summers. The annual average

Fig. 1 False-composite image (ASTER bands, Reiche et al. 2012b) of the investigation site in Inner Mongolia, China
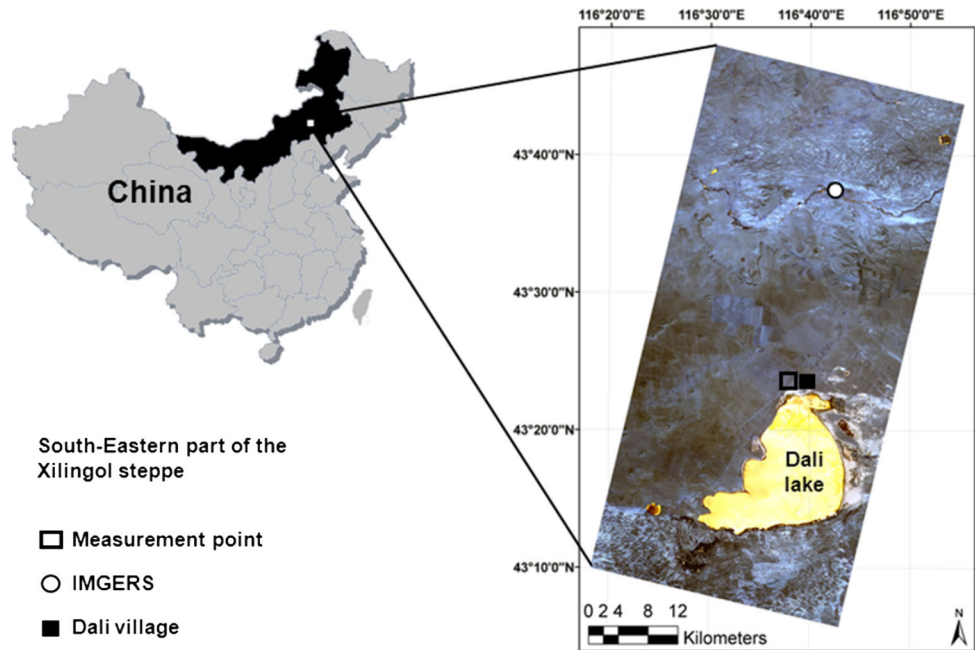
temperature is 0.7 °C and the precipitation rate is 335 mm [representative for the period from 1982 to 2005 at IM-GERS (Inner Mongolian Grassland Research Ecosystem Station) managed by the Institute of Botany of the Chinese Academy of Sciences] (Schaffrath et al. 2011). More than 70 % of the precipitation falls between May and August. Wind erosion occurs from mid-March to mid-May (Shinoda et al. 2010) caused primarily by westerly winds. A monthly maximum wind velocity occurs in April and May with averages of 11.5 and 10.4 km h^{-1} (annual average = 8.6 km h^{-1}) (FAO 2001). The low vegetation cover in spring, which mainly consists of the dead vegetation from the previous year, a low precipitation rate and high wind velocities from directions between northwest to southwest cause numerous dust storms.

In recent years, large areas of the Xilingol steppe were seriously degraded by overgrazing, which led to noticeable changes in topsoil properties (Krümmelbein et al. 2009; Kölbl et al. 2011). Degraded soils are more vulnerable to wind erosion. This results in huge amounts of soil loss and triggers desertification processes (Hoffmann et al. 2011). Reiche et al. (2012b) estimated that about 75 % of the region is covered by typical grassland subdivided into three classes with regard to its degree of degradation. Grassland classified as highly degraded accounts for 26 %, while the largest part with moderately and less degraded grassland covers an area of 41 and 8 %, respectively. Arable land and open surfaces (dunes, bare soil and salt pans, coverage by gravel only at the very top of volcanoes) account for about 6 and 4 %, respectively. Although small in area, arable land contributes extraordinarily to the dust emissions of the

region. Estimates in the Xilingol steppe in 2006 resulted in 75 % of the total dust emissions originating from the arable land (5 % of the area) and only 25 % of the dust emissions from the grassland (95 % of the area). This quantification is based on Hoffmann et al. (2011).

The predominant soil types in the Xilingol steppe are classified as Phaeozem, Chernosem and Arenosol (Barthold et al. 2013) above acid volcanic rocks (WRB 2006). More than 50 % of the soil consists of fine sand and coarse silt, a strong indication of aeolian contribution at these soil formations (Hoffmann et al. 2008a). The loamy to sandy soil texture varies in the sand fraction between 45 and 64 %, in silt between 18 and 29 % and in clay between 18 and 27 % (Kölbl et al. 2011). The highest sand and lowest clay content of about 68 and 12 % is recognized in heavily grazed areas (Krümmelbein et al. 2009).

Dust fluxes regarded at landscape scale

The soil cover up to 25–35 km in front of the measuring point was taken from a former analysis of source/sink patterns of dust in the area to explain the measured dust concentration gradients and dust size distribution in the context of the windward landscape structure (Reiche et al. 2012b). This distance seems to be far enough to compensate for changes in the internal boundary layer caused by surface roughness changes in that region and to include both local (0–10 km) and regional dust sources (10–1,000 km) (Lawrence and Neff 2009). At landscape scale the study addresses a wide range of natural features
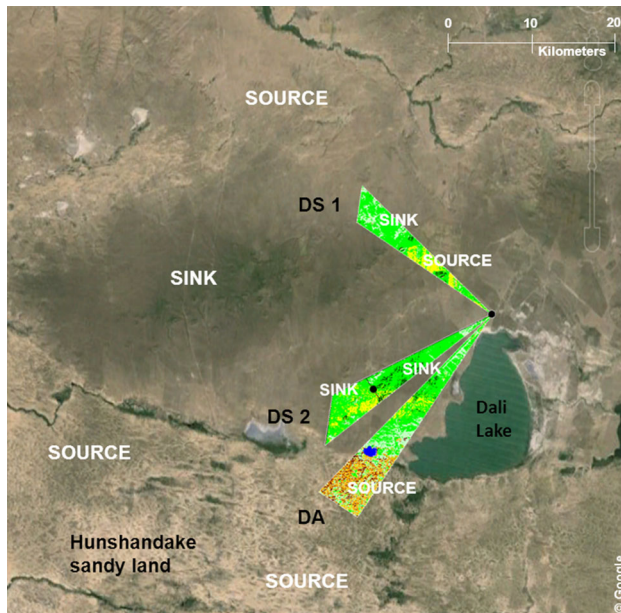
Fig. 2 Analysed sectors in windward directions of the measurement point by dust event. Length of sectors is determined by ASTER data used from Reiche et al. (2012b) (*dark green* ungrazed, *light green* moderate grazed, *grey–green* heavily grazed, *yellow* arable land, *dark yellow* bare soil/dunes, *brown* bushes, *blue* water)

(dunes, lakes) and human-induced changes in land use/cover decisions. Generally, wind erosion/deposition processes are highly variable and heterogenous and not limited to one ecosystem or river catchment.

The basic assumption is that the dust concentration profile will reflect the properties of the crossed landscape structures acting as source or sink areas. The transported finer fractions of dust in suspension mode are less affected by landscape structure changes. Coarser fractions

emitted from the immediate surroundings and transported in saltation or short-term suspension mode are more affected with regard to the emission/deposition processes. Therefore, sectors in windward direction of the measurement point were analyzed regarding their landscape structure (Fig. 2). An opening angle of 10° takes wind direction changes into account during the kite ascent. Topography and grass height are the main factors for deposition or emission processes in grassland (Hoffmann et al. 2008a). The landscape in all windward directions from the measurement point was mainly flat to undulating and thus, the separation in sink and/or source areas along the transport path was determined by differences in vegetation height (using the critical grazing intensity following Hoffmann et al. 2008a). In each sector the land use/cover was classified, e.g., ungrazed, moderately and heavily grazed areas, arable land, bare soil, water/ice and bushes by an remote sensing/GIS approach (ArcView3.2, ESRI) (Reiche et al. 2012b).

Measurement of dust fluxes and flux calculations

Dust concentrations were measured at a grassland site north of the Dalai Nur Lake from the end of April to the beginning of May in 2011 using a kite to carry dust measurement equipment up to heights of several decameters. Six dust events were investigated with the kite-borne system. The utilised method is explained in detail by Reiche et al. (2012a). Key advantages of the system are its compact size, robustness and mobility and its easy handling with minimum manpower. Further, the system requires no time-consuming assembly and disassembly and can therefore be used at a much wider range of sites compared to monitoring towers.

Fig. 3 Kite-based dust profiling system (**a**) and ground station (**b**) for simultaneous measurement
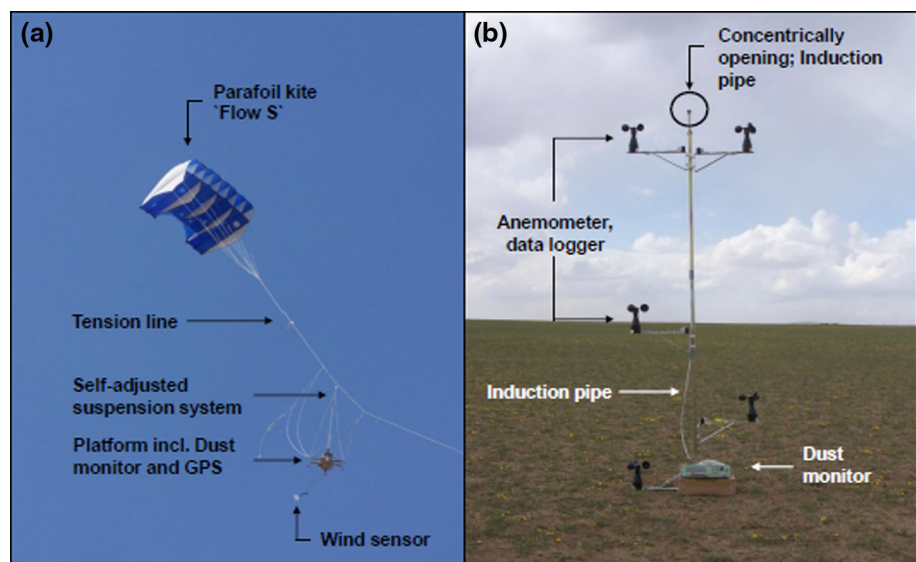
Table 1 Dust storm classification (modified after Hoffmann et al. 2008a)

Category	Classification		
	Visibility (m)	PM_{10} (hourly average) ($\mu g\ m^{-3}$)	Wind velocity[a] (ms^{-1})
Dusty air			
DA	>2,000	50–200	–
Light dust storm			
DS 1	<2,000	200–500	–
Dust storm			
DS 2	<1,000	500–2,000	>17
Strong dust storm			
DS 3	<200	2,000–5,000	>20
Serious dust storm			
DS 4	<50	>5,000	>25

[a] Following Central Weather Bureau (CWB, China)

Particle mass and particle number concentrations were measured simultaneously by two environmental dust monitors (EDM, GRIMM Aerosol Technique, Germany), one carried by a kite-borne system to different heights (Fig. 3a, self-adjusting measurement platform) and the other installed at 2 m height as surface reference (Fig. 3b). The EDM sucks in the air continuously through an omnidirectional introduction pipe with a rate of 1.2 l min^{-1}. Particles in the air sample passed a laser light and were counted and classified in 30 size classes between 0.25 and 32 μm. Then the particle counts were grouped in classes and converted to PM_1, $PM_{2.5}$ and PM_{10} as mass concentration ($\mu g\ m^{-3}$) and the data saved at a time interval of 6 s. The capture-efficiency of the EDM was calibrated in wind tunnel runs comparing isokinetic inlets with omnidirectional inlets to correct the measured data even above wind velocities which were not considered by the producer. PM mass concentrations had to be corrected by 16 % for wind velocities between ≤12 and ≤17 ms^{-1} and by 21 % above 17 ms^{-1}. Up to 12 ms^{-1} the loss of PM is less than 10 % and therefore negligible (producer's declaration). The measured particle numbers (n per liter) were used to calculate the mass of each particle class using Eq. (1):

$$M = \frac{4}{3}\pi r^3 \rho, \tag{1}$$

where ρ is the particle density (2.65 Mg m^{-3}) and r is the radius.

Three measuring heights with $z_1 = 20–30$ m, $z_2 = 40–50$ m and $z_3 = 70–80$ m were chosen for the kite system according to one-third, two-thirds and full-length of the kite line. The kite position was recorded by a GPS with tracking function (GPS 60^{TM}, GARMIN Ltd., USA). The wind velocity was measured at kite height by a self-adjusting propeller anemometer (Bräuniger Ltd., Germany) and at ground level with a set of cup anemometers at 0.15, 0.5, 1 and 2 m (Thies Climate GmbH, Germany). Wind data were sampled simultaneously to the particle counts every 6 s in the EDM at kite level, and additionally by four micro data loggers at ground level (irDAN®pulse, ESYS Company, Germany). The latter were used to calculate the friction velocity $u*$ and the surface roughness length z_0.

The vertical dust flux, F_V ($\mu g\ m^{-2}\ s^{-1}$) of PM_1 and PM_{10} were calculated according to Gillette (1977) with:

$$F_V = \frac{u \times k \times (c_1 - c_2)}{\ln\left(\frac{z_2}{z_1}\right)}, \tag{2}$$

where u is the wind velocity at height (ms^{-1}), k is the von Kàrmàn constant of 0.41, c_1 and c_2 are the PM concentrations ($\mu g\ m^{-3}$) at height z_1 (on ground at 2 m height) and height z_2 of the EDM lifted by kite in (m).

The measured dust concentrations used in the study cover a spectrum between dusty air to strong dust storm following the 'dust storm classification' of the Central Weather Bureau of China modified by Hoffmann et al. (2008a) (Table 1).

Results

Characterization of the gradient measurements

Dust gradients were measured between the reference in 2 m height and the flight altitude of the kite in about 25, 45

Table 2 Changes of dust concentration with height ($\Delta c/\Delta z$) of PM_{10} and PM_1 of each dust event

Δz[a]	Δc[b] (PM_{10}, µg m)			Δc (PM_1, µg m)		
	DS 1[c]	DA[c]	DS 2[c]	DS 1	DA	DS 2
75	0.5 (0.4/0.6)			0.07 (0.05/0.08)		
45	2.6 (0.2/0.5)	−3.6 (−3.0/−4.2)	8.4 (5.9/10.8)	0.12 (0.12/0.12)	−0.05 (−0.02/−0.07)	−0.13 (0.05/−0.31)
25	9.7 (0.2/19.3)	−5.5 (−4.5/−6.5)	20.0 (19.6/20.5)	0.33 (0.27/0.38)	−0.12 (−0.04/−0.20)	−0.92 (0.83/1.01)

[a] Approximate height difference

[b] Changes in dust concentration with height

[c] Dust storm category, see Table 1

Table 3 Weather data at ground station during observation period at the catchment site

Date/dust event[a]	Time[b] (local) (h:mm)	Average/maximum wind velocity[c] $u_{av/max}$ (ms^{-1})	Wind direction	Stable roughness length[d] z_{0av} (m)	Friction velocity[d] $u*_{av}$ (ms^{-1})
May 8th/dust storm 1 (DS 1)	9:30–11:30 AM	7.4 ± 0.9/9.7	NW	0.0029/0.0032/0.0031	0.47/0.48/0.44
May 8th/dusty air (DA)	1:45–3:45 PM	9.3 ± 1.2/12.9	SW	0.0047/0.0027	0.65/0.56
May 11th/dust storm 2 (DS 2)	7:15–9:15 AM	11.0 ± 1.5/15.1	W–SW	0.0059/0.0075	0.73/0.83

[a] Dust storm category, see Table 1

[b] Time including assembly and dismantling

[c] Average and maximum wind velocity at time at 6 s interval

[d] Wind velocity as average at 0.15, 0.5, 1 and 2 m height are used in Eq. (2)

Table 4 Variations during recording period, average and maximum wind velocity using the kite-borne system

Date/dust event[a]	Kite profiling (min) at height z (m)[b]			Total time (min)	Average/maximum wind velocity (ms^{-1}) at height z (m)[b]		
	z (1) 20–30	z (2) 40–50	z (3) 70–80		u_{max} z (1)	u_{max} z (2)	u_{max} z (3)
May 8th/DS 1	10	20	10	40	12.0 ± 1.8/17.3	12.9 ± 2.1/18.6	14.4 ± 1.8/18.5
May 8th/DA	20	15	–	35	15.4 ± 2.0/19.2	16.9 ± 2.6/21.6	–
May 11th/DS 2	10	15	–	25	16.7 ± 2.0/21.4	18.4 ± 2.3/24.6	–
Total time				135			

[a] Dust storm category, see Table 1

[b] Range of realized kite heights

and 75 m. These height differences were sufficient to measure dust concentration differences outside the measurement error and to derive the direction of the vertical fluxes with certainty (Table 2). A detailed description of dust event characterizations, measured dust concentrations and ratios of specific size classes are presented in Tables 3, 4 and 5.

Light dust storm event

A 'light dust storm' (DS 1) crossed the observation site in the morning of May 8th arriving from northwest. The average wind velocity at 2 m height was 7.4 ms^{-1} with friction velocities ranging from 0.44 to 0.48 ms^{-1} (Table 3). The wind velocity remained below the threshold to initiate wind erosion in moderately grazed grassland, but was close above the threshold for arable land of 7.2 ms^{-1} (Zhang et al. 2012). Dust measurements with the kite-borne system were made at all three heights (Table 4). PM$_{10}$ concentrations at the reference height of 2 m decreased from 264 to 125 μg m^{-3} correlating with decreasing wind velocity. The concentrations at each height of the kite-borne system remained constant at 85–89 μg m^{-3}. The measured PM$_{10}$ concentrations clearly show an emission process which can be attributed to arable land, while the PM$_1$ concentrations with about 30 μg m^{-3} show no significant differences with changing measuring height and dust concentrations (Table 5).

Dusty air event

In the course of the day the measured concentration showed a gradual decrease from 'light dust storm' (DS 1) in the morning to 'dusty air' (DA) in the early afternoon in combination with an increase of the average wind velocity at the reference station to 9.3 ms^{-1} in the wind direction. The corresponding friction velocity shows significantly higher values of 0.56 and 0.65 ms^{-1} (Table 3). The wind direction changed from northwest (DS 1) to southwest resulting in a new catchment area with different landscape structure concerning characteristics for emission or deposition of dust (Fig. 2). Additionally, peaks in wind velocity exceeded the threshold for wind erosion at grassland, so that these areas can be regarded as an occasional source (Zhang et al. 2012). The PM$_{10}$ concentration at ground remains constant at about 100 μg m^{-3} while the dust concentration at both measurement heights z_1, 20–30 m and z_2, 40–50 m increased to about 250 μg m^{-3} (Table 5). That is a first clear indication of dust from remote source areas settling down during the passage of the grassland. Similar to DS 1, the PM$_1$ concentration showed no significant variability with increasing measuring height (Table 5).

Strong dust storm event

A supra-regional 'dust storm' (DS 2), with origin in the Gobi desert, crossed the observation site from west to

Table 5 PM size concentrations and PM ratios measured by reference station (REF) on ground and using the kite-borne dust profiling system (KIDS)

| Date/dust event[a]	Height z (m)	Average PM$_{10}$[b] (µg m^{-3})		Average PM$_1$[b] (µg m^{-3})		PM:PM ratios			
		PM$_{10,REF}$	PM$_{10,KIDS}$	PM$_{1,REF}$	PM$_{1,KIDS}$	PM$_{10,REF}$:PM$_{10,KIDS}$	PM$_{1,REF}$:PM$_{1,KIDS}$	PM$_{10}$:PM$_{1,REF}$	PM$_{10}$:PM$_{1,KIDS}$
May 8th/DS 1	z_1 20–30	264 ± 212	85 ± 36	32 ± 2	26 ± 3	3.1	1.2	8.3	3.3
	z_2 40–50	196 ± 133	86 ± 35	31 ± 2	26 ± 2	2.3	1.2	6.3	3.3
	z_3 70–80	125 ± 42	89 ± 33	30 ± 1	25 ± 2	1.7	1.2	4.2	3.6
May 8th/DA	z_1 20–30	117 ± 22	256 ± 48	29 ± 1	32 ± 3	0.5	0.9	4.0	8.0
	z_2 40–50	103 ± 21	257 ± 47	30 ± 2	32 ± 3	0.4	0.9	3.4	8.0
May 11th/DS 2	z_1 20–30	932 ± 94	476 ± 83	88 ± 6	67 ± 8	1.9	1.3	10.6	7.2
	z_2 40–50	1,075 ± 138	747 ± 234	90 ± 9	95 ± 16	1.4	0.9	11.9	7.9

[a] Dust storm category, see Table 1

[b] PM size concentration as average value simultaneously measured on ground and by kite height

south-western direction on May 11th. This event was documented by satellite images (http://earthobservatory.nasa.gov/NaturalHazards/event.php?id=50565). Measurements began immediately in the morning as the dust storm began. The average wind velocity of 11 ms^{-1} and wind peaks >15 ms^{-1} near ground corresponded with high friction velocities of 0.73 and 0.83 ms^{-1} (Table 3). The average wind velocity was well above the threshold for bare soil or dunes located further away, and just below the threshold for wind erosion on moderately grazed grassland in the surroundings (12.8 ms^{-1}), while the maximum peaks exceeded this threshold. Relatively constant discharge of material from the dust storm and additional fluctuating emissions of local wind erosion was expected. The PM$_{10}$ concentration profiles of 932–1,075 µg m^{-3} at ground and 476–747 µg m^{-3} (Table 5) at kite heights already indicated upward-directed fluxes (dust emission), while PM$_1$ concentrations slightly increased with height within the measurement error (Table 5).

Dust composition

The particle number and particle mass concentrations (calculated by Eq. 1) of the 30 particle size classes are shown in Fig. 4. Both, particle number and mass distribution, significantly differ between the dust storm intensities. The mass concentration at both measuring heights of DS 1 has a bimodal distribution with a maximum in coarser particle diameters of 20–25 µm and a second maximum at 5–6.5 µm (Fig. 4a). The mass of particles >20 µm accounts for about 45 % of the total mass. The DA event has a maximum at diameters of 3–3.5 µm with a general higher concentration at the kite heights than at ground. The size composition of the DA dust generally consists of finer fractions (Fig. 4b). Despite higher wind velocities, wind erosion in the surrounding areas can be excluded and the measured profiles are similar to the dust advection situation as described by Park et al. (2013). The particle mass >20 µm is about 20 %, showing a distinct reduction of the short-term suspension load by deposition processes along the grassland.

DS 2 as a supra-regional dust storm (Gobi as source region) with local effects has different distributions of the transported particle sizes depending on the measuring height. At ground, a unimodal distribution with its maximum at 4–5 µm was observed, which represents the decrease in the relative abundance in frequency of coarser particles with greater distance to the dust source area (Lawrence and Neff 2009). Contrary to this, the particle-size distribution at the kite levels was bimodal with a second maximum of the coarser particles between 17 and 20 µm (Fig. 4c).
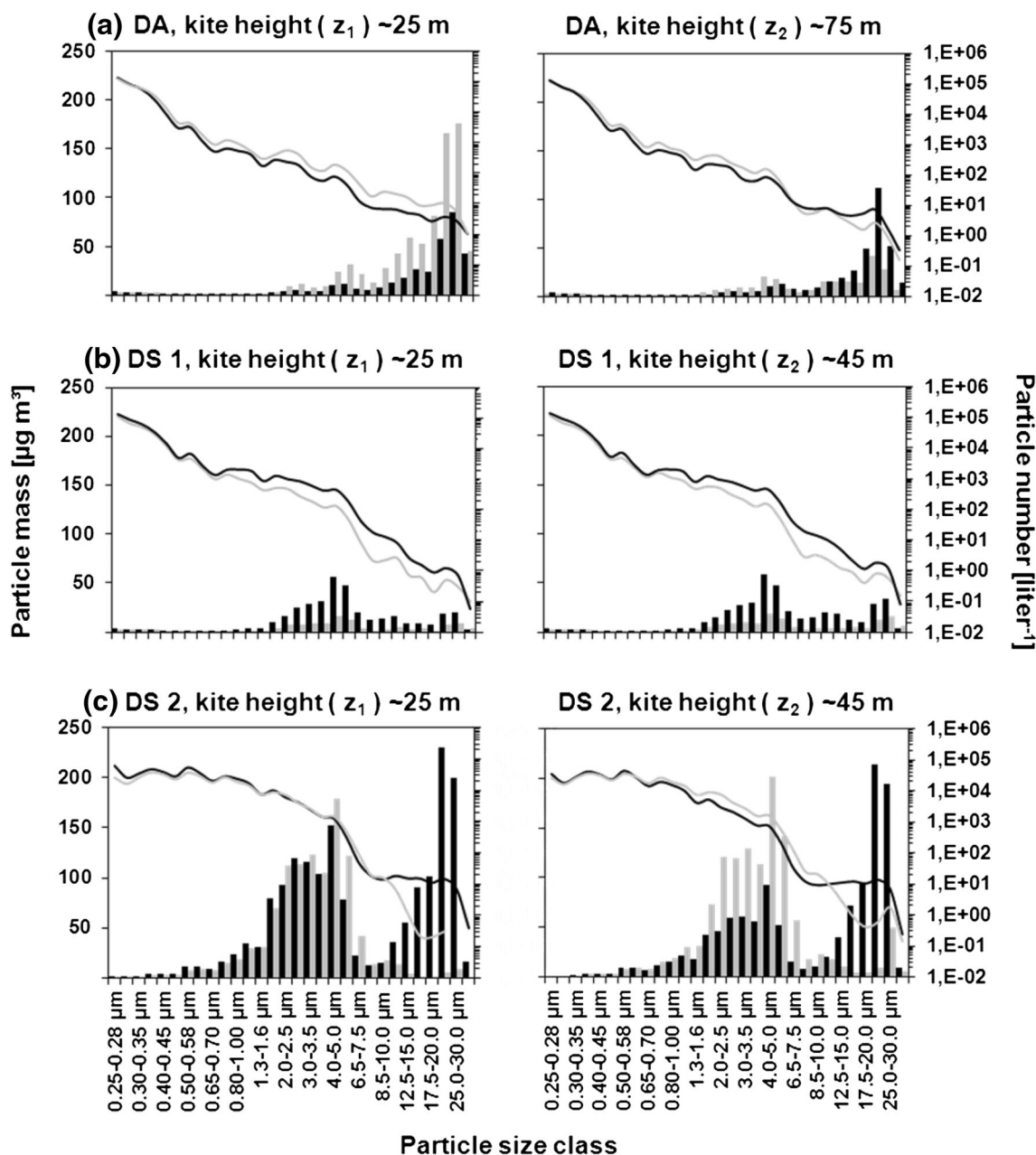
Fig. 4 Particle-number and particle-size distribution of parallel measurements. *Grey curves* and *bars* are results of the ground station and *black curves* and *bars* belong to the kite-borne system. Particle size classes on *x* axis are depicted for every second class

Derivation of vertical fluxes

The average concentrations of PM_{10} and PM_1 measured near ground at 2 m height and corresponding heights by the kite-borne system were used to estimate the vertical fluxes between both points with Eq. (2) (Table 5). In contrast to PM_{10}, concentrations of PM_1 show no significant changes at the measured heights. Positive values represent upward fluxes of the corresponding PM class, negative values downward fluxes (Table 6). Dust concentrations at ground and kite heights clearly indicate emission processes at DS 1

and DS 2, compared to DA where deposition processes can be derived (Table 6). Further, the calculated gradients ($\Delta c/\Delta z$, Table 2) of dust concentration with a related variability (measurement error) for each category finally, provide an initial indication of the direction in dust fluxes.

Influence of land use/cover on dust fluxes

The sector analysis provides the proportion of source/sink areas within the sector in front of the measurement point (Figs. 2, 5). For the DS 1 event from northwest direction,

Table 6 Vertical dust flux (F_V) of PM_{10} and PM_1 fraction between ground and measured kite height

| Date/dust event[a]	Number of kite profile	PM_{10}, $F_V^{[b]}$ ($\mu g\ m^{-2}\ s^{-1}$)	PM_1, $F_V^{[b]}$ ($\mu g\ m^{-2}\ s^{-1}$)
May 8th/DS 1	1	14.97	0.48
	2	7.06	0.30
	3	1.83	0.23
May 8th/DA	1	−14.17	−0.24
	2	−11.31	−0.20
May 11th/DS 2	1	54.26	2.64
	2	37.69	−0.53

[a] Dust storm category, see Table 1

[b] F calculated between 2 m and z_{1-3} of kite height

25 km in front of the measuring point were analyzed. About 31 % of the area can be considered as source for dust, including arable land (17 %), heavily grazed grassland (13.5 %) and dunes (0.5 %). Sinks are mainly moderately grazed areas (66 %) located further away from the measurement point, while the source areas are closer (5–10 km) to the measurement point. The sector of DA (from southwest direction, 35 km in length) can be divided in two parts, a large dune belt about 30 km away (120 km in width, which can be regarded as considerable dust source, outside the analyzed image) and grassland representing changing source/sink patterns (Fig. 2). Here, source areas dominate with about 57 %, mainly arable land and tracks. The sector of the DS 2 event (from west to southwest direction, 25 km in length) has the highest proportion of sink areas (80 %) represented by moderately grazed grassland. Source areas are arable land (12 %, placed in the middle of the sector) and small overgrazed areas (6 %). A correlation between the percentage of dust source areas in each sector and the calculated vertical dust fluxes of PM_{10} showed good matches (Fig. 6).

Discussion

The study aimed to be a first approach to relate measured dust concentration gradients to land use/land cover in a wider scale and to continue measurements by Hoffmann et al. (2008a) that examined the vertical distribution of fine dust concentration above grassland close to the ground. The measured gradients ($\Delta c/\Delta z$) close to the ground were too small to detect upward or downward fluxes with certainty, i.e., whether the area can be regarded as sink or source for dust remained uncertain. One possibility to overcome these limitations is to measure horizontal fluxes in greater height differences. The use of a kite-borne system (Reiche et al. 2012a) enables measurements with
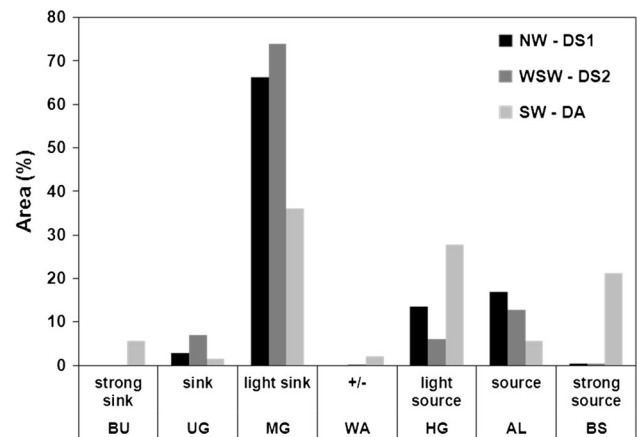
Fig. 5 Proportion of dust source/sink areas within the sectors (*BU* bushes, *UG* ungrazed, *MG* moderate grazed, *WA* water, *HG* heavily grazed, *AL* arable land, *BS* bare soil)
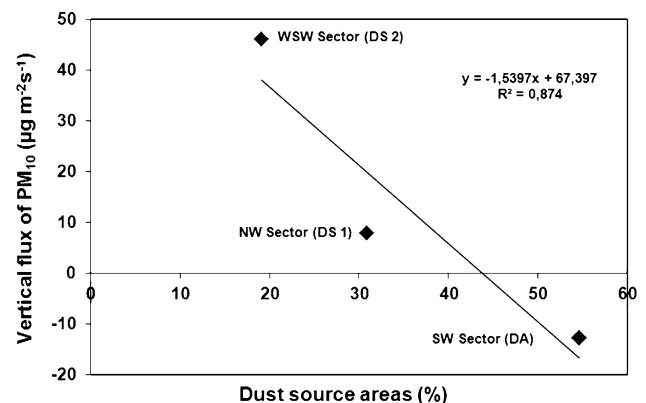
Fig. 6 Correlation between vertical dust fluxes (average over the height) and dust source in each sector

sufficient height differences of dust concentrations to derive vertical fluxes with the required degree of certainty.

Three different dust events from a number of directions were measured and classified according to the dust storm classification by Hoffmann et al. (2008a). The three dust events represented dust storm categories between 'dusty air' to 'strong dust storm'. Structures of land use/cover in windward direction of the measuring point were analyzed. This resulted in different source/sink patterns and had to be taken into account for the interpretations of height depending on PM concentration and particle size composition.

The relatively high PM_{10} concentration and coarser particle sizes of the DS 1 event were caused by local wind erosion in windward direction, since the dust most likely originated from arable land 5–10 km away (Reiche et al. 2012b) (Fig. 2). The dust from local sources mainly consists of fine silt (2–20 μm) and coarse silt (>20–50 μm)

fractions. The predominant transport mode of these fractions can be regarded as short-term suspension (Shao 2000). This is confirmed by the measured dust composition and the derived flux direction (emission). Coarser particles (>20 μm) tend to deposit closer to the source (Rea and Hovan 1995; Lawrence and Neff 2009). In the case of DS 1, the distance from the source area was not sufficient for deposition of the complete coarse dust load since particle mass dominated even at the kite height of 75 m.

On the same day the wind direction changed at about 90° from northwest to southwest resulting in a new dust storm category (DA) with regard to wind velocity and dust concentration. Source or sink areas in front of the measuring point changed considerably since the wind crossed a large dune belt with an extent of about 120 km before entering moderate grazed grassland of about 30 km length. The dune belt (Hundhandake sandy land, Fig. 2) is severely disturbed by overgrazing with large parts of bare soil highly susceptible to wind erosion (Reiche et al. 2012b). Dunes mainly contain sand particles and the dust is produced by collisions of these grains (Okin 2005). The produced dust is much finer than dust from the arable land as estimated in DS 1. Larger particles of the silt-size fractions which are emitted in the dune field settle down during the much longer passage over the grassland. The relationship between the potential deposition rate and the distance to the dust source area described by Lawrence and Neff (2009) is reflected by the particle composition. The comparison of particle-size distributions of both dust events, DS 1 and DA, indicates that DS 1 can be classified as a local dust event, whereas DA reflects the characteristics of regional dust events. These results could additionally be confirmed by the transport distance between the source areas and the measurement point. Further, a similar particle-size distribution had been observed in the Horqin desert, where the same emission processes occur and the dust composition was very similar (Park and Park 2014).

The DS 2 event originated in the Gobi desert and carried a huge amount of fine sand and dust as long-range transport. Wind erosion occurred due to the high wind velocity in the dunes and adjacent grassland, which acts as an additional source. The particle size composition at the DS 2 event significantly differs on ground and at the kite heights. At ground, the concentration of finer particles is higher. The particle sizes show a normal distribution near ground with maximum particle sizes of 2–3 μm, and can be regarded as background dust which is transported over thousands of kilometers (Grousset et al. 2003, Zhao et al. 2006). According to a study by Tsoar and Pye (1987) particle size decreases with increasing distance to the source during supra-regional dust storm events. Thus, it can be assumed that the PM particles measured in this study originated from far away. In contrast, the particle-size

distribution at kite heights shows a clear bimodal distribution in particle size composition. In addition to the background dust with a maximum of particles in fractions between 2 and 4 μm, local and/or regionally emitted particles are reflected by greater particle sizes of >10 μm. Although the grassland is in good condition, the strong wind velocities caused additional dust emissions. A further hint is the high standard deviation of PM_{10}, which is a result of the discontinuous contribution of wind erosion by the fluctuating wind velocities around the threshold value of about 13 ms^{-1}.

The measured particle mass and size concentrations reflect different dust sources from supra-regional, regional and local sources. The interactions of wind erosion, dust emission and dust deposition could be explained by the particle size compositions. Because of the interaction/mixture of all wind erosion processes, a separate consideration of the particle size classes (smaller and greater than PM_{10}) is useful. For the single particle size classes, DS 2 shows two opposite directions of the fluxes, emission flux for size classes <10 μm and deposition for all particles >10 μm. The ratios of PM_{10}/PM_1 (Table 5) are typical for dust storms as could be also found in other regions (Shahsavani et al. 2012; Park et al. 2013).

Generally, dust emission/deposition processes are highly variable and not restricted to an ecosystem or catchment. This is reflected by the extent of local (0–10 km) and regional (10–1,000 km) scales of the contributing processes (Lawrence and Neff 2009). The length of about 30 km chosen for the land use classification of this study covers the local scale, whereas the complete regional scale could be regarded in a study like this. But, the main characteristics of possible source areas, as arable land or sand dunes, could be detected and differentiated by the measurements. The grassland is mainly a deposition area, even in early spring when most of the vegetation canopy is dead.

Conclusion

Grassland ecosystems like the semi-arid Inner Mongolian grasslands developed under the impact of regular dust depositions from large dust source regions hundreds of kilometers away.

To understand whether grazing has changed the basic characteristics of grassland as a sink to a source area of aeolian dust, it is necessary to detect differences in horizontal dust fluxes to precisely derive the direction of vertical fluxes. For this purpose, measurements in greater height differences are needed. In the present study, these measurements were realized in three height differences by a kite-borne system.

The measured particle mass and number concentrations at ground and additionally in 25, 50 and 75 m aimed to support the determination of vertical dust fluxes. The extension of the measurements at ground enabled a more precise identification of the flux direction, which is usually carried out in the first few meters and from which a precise determination of the vertical dust flux direction was difficult (Hoffmann et al. 2008a).

While the flux direction indicated whether the grassland functions as source or sink, the particle size made it possible to determine the distance of the potential source from the measurement location. Particle sizes differ according to the origin and the process of dust release. Greater particle size classes (>10 μm) mainly indicate dust sources in the surroundings (local erosion, <10 km), whereas small size classes usually originate from sources far away. Therefore, the particle-size distribution is one means to separate dust emitted from local and regional sources.

The study constitutes a first approach using dust measurements and land use patterns on a larger scale to classify dust emission or deposition processes in semi-arid grasslands. Although the results confirmed the applicability of this approach, additional measurements are needed to improve and elaborate the methodology.

References

Alfaro S (2008) Influence of soil texture on the binding energies of fine mineral dust particles potentially released by wind erosion. Geomorphology 93:157–167

Andreae MO (1995) Climate effects of changing atmospheric aerosol levels. In: Henderson-Sellers A (ed) World survey of climatology 14. Future climates of the world—a modelling perspective. Elsevier, Amsterdam, pp 341–392

Angerer J, Han GD, Fujisaki I, Havstad K (2008) Climate change and ecosystems of Asia with emphasis on Inner Mongolia and Mongolia. Ranglands 30:46–51

Balsley BB, Jensen ML, Frehlich RG (1998) The use of state-of-art kites for profiling the lower atmosphere. Bound Layer Meteorol 87:1–25

Barthold F, Wiesmeier M, Breuer L, Frede HG, Wu J, Blank FB (2013) Land use and climate control the spatial distribution of soils in the grasslands of Inner Mongolia. J Arid Environ 88:194–205

Butterbach-Bahl K, Kögel-Knabner I, Han XG (2011) Steppes ecosystems and climate and land-use changes—vulnerability, feedbacks and possibilities for adaption. Plant Soil 340:1–6

Chen SP, Bai YF, Lin GH, Liang Y, Han XG (2005) Effects of grazing on photosynthetic characteristics of major steppe species in the Xilin River Basin, Inner Mongolia, China. Photosynthetica 43:559–565

Dong Z, Man D, Luo W, Qian G, Wang J, Zhao M, Liu S, Zhu G, Zhu Z (2010) Horizontal aeolian sediment flux in the Minqin area, a major source of Chinese dust storm. Geomorphology 116:58–66

FAO (2001) World-wide agroclimatic database. FAOCLIM 2. Environmental and Natural Resources Service, Agrometeorology Group, FAO, Rome

Fryrear DW (1986) A field dust sampler. J Soil Water Conserv 41:117–120

Funk R, Li Y, Hoffmann C, Reiche M, Zhang Z, Li J, Sommer M (2012) Using ^{137}Cs to estimate wind erosion and dust deposition on grassland in Inner Mongolia—selection of a reference site and description of the temporal variability. Plant Soil 351:293–307

Funk R, Hoffmann C, Reiche M (2013) Methods for quantifying wind erosion in steppe regions. In: Mueller L, Saparov A, Lischeid G (eds) Novel measurement and assessment tools for monitoring and management of land and water resources in agricultural landscapes of Central Asia. Springer International Publishing, Dordrecht, pp 315–327

Gillette DA (1977) Fine particulate-emission due to wind erosion. Trans ASAE 20:890–897

Goossens D (2006) Aeolian deposition of dust over hills: the effect of dust grain sizes on deposition pattern. Earth Surf Process Landf 31:762–776

Goossens D, Offer ZY (2000) Wind tunnel and field calibration of six aeolian dust samplers. Atmos Environ 24:1043–1057

Grousset FE, Ginoux P, Bory A, Biscaye PE (2003) Cas study of a China dust plume reaching the French Alps. Geophys Res Lett 60:1277. doi:10.1029/2002GL016833

Herman JR, Bhartia PK, Torres O, Hsu C, Seftor C, Celarier E (1997) Global distribution of UV-absorbing areosols from Nimbus 7/TOMS data. J Geophys Res 102:16911–16922

Hoffmann C, Funk R, Wieland R, Li Y, Sommer M (2008a) Effects of grazing and topography on dust flux and deposition in the Xilingele Grassland, Inner Mongolia. J Arid Environ 72:792–807

Hoffmann C, Funk R, Sommer M, Li Y (2008b) Temporal variations in PM$_{10}$ and particle size distribution during Asian dust storms in Inner Mongolia. Atmos Environ 42:8422–8431

Hoffmann C, Funk R, Reiche M, Li Y (2011) Assessment of extreme wind erosion and its impacts in Inner Mongolia, China. Aeolian Res 3:327–342

IPCC (2013) Climate Change 2013. The physical science basis. Contribution of Working Group I to the Fifth Assessment Report of the Intergovernmental panel on climate change. In: Stocker TF, Qin D, Plattner GK, Tignor M, Allen SK, Boschung J, Nauels A, Xia Y, Bex V, Midgley PM (eds). Cambridge University Press, Cambridge, p 1535

Kölbl A, Steffens M, Wiesmeier M, Hoffmann C, Funk R, Krümmelbein J, Reszkowska A, Zhao Y, Peth S, Horn R, Giese M, Kögel-Knabner I (2011) Grazing changes topography-controlled topsoil properties and their interaction on different spatial scales in a semi-arid grassland of Inner Mongolia, P.R. China. Plant Soil 340:35–58

Krümmelbein J, Perth S, Zhao Y, Horn R (2009) Grazing-induced alterations of soil hydraulic properties and functions in Inner Mongolia, PR China. J Plant Nutr Soil Sci 172:769–776

Lawrence CR, Neff JC (2009) The contemporary physical and chemical flux of aeolian dust: a synthesis of direct measurements of dust deposition. Chem Geol 267:46–63

Lee H, Tanaka H, Chiba M, Igarashi Y (2003) Long range transport of Asian dust from dust storms and its impact on Japan. Water Air Soil Pollut 3:231–343

Li SG, Harazono Y, Oikawa T, Zhao HL, Ying Z, Chang XL (2000) Grassland desertification by grazing and resulting micrometeorological changes in Inner Mongolia. Agric For Meteorol 102:125–137

McGowan HA, Clark A (2008) A vertical profile of PM_{10} dust concentration measured during a regional dust event identified by MODIS Terra Western Queensland. Australia. J Geophys Res 113:F02S03

McTanish G, Chan GY, McGowan HA, Leys J, Tews K (2005) The 23rd October 2002 dust storm in eastern Australia: characteristics and meteorological conditions. Atmos Environ 39:1227–1236

Okin GS (2005) Dependence of wind erosion and dust emission an surface heterogeneity: stochastic modeling. J Geophys Res 110:D11

Park SU, Park MS (2014) Aerosol size distribution observed at Naiman in the Asian dust source region of Inner Mongolia. Atmos Environ 82:17–23

Park SU, Cho JH, Park MS (2013) Identification of visibility reducing weather phenomena due to aerosols. Environ Manag Sustain Dev 2:126–142

Prospero JM, Ginoux P, Torres O, Nicholson SE, Gill TE (2002) Environmental characterisiation of global sources of atmospheric soil dust identified with the Nimbus 7 total ozone mapping spectrometer (TOMS) absorbing aerosol product. Rev Geophys 40:2–32

Rea DK, Hovan SA (1995) Grain-size distribution and distribution processes of the mineral component of abyssal sediments—lessons from the North Pacific. Paleoceanography 10:251–258

Reiche M, Funk R, Zhang Z, Hoffmann C, Li Y, Sommer M (2012a) Using a parafoil kite for measurement of variations in particulate matter—a kite-based dust profiling approach. J Atmos Clim Sci 2:41–51

Reiche M, Funk R, Zhang Z, Hoffmann C, Reiche J, Wehrhan M, Li Y, Sommer M (2012b) Application of satellite remote sensing for mapping wind erosion risk and dust emission-deposition in Inner Mongolia grassland, China. Grassl Sci 58:8–19

Schaffrath D, Barthold FK, Bernhofer C (2011) Spatiotemporal variability of grassland vegetation cover in a catchment in Inner Mongolia, China, derived from MODIS data products. Plant Soil 340:181–198

Shahsavani A, Naddafi K, Haghighifard NJ, Mesdaghinia A, Yunesian M, Nabizadeh R, Arahami M, Sowlat MH, Yarahmadi M, Saki H, Alimohamadi M, Nazmara S, Motevalian SA, Goudarzi G (2012) The evaluation of PM10, PM2.5, and PM1 concentrations during the Middle Eastern Dust (MED) events in Ahvaz, Iran, from April through September 2010. J Arid Environ 77:72–83

Shao Y (2000) Physics and modelling of wind erosion. Kluwer Academic Publishers, London

Shinoda M, Kimura R, Mikami M, Tsubo M, Nishihara E, Ishizuka M, Yamanda Y, Munkhtsetseg E, Jugder D, Kurosaki Y (2010) Characteristics of dust emission on the Mongolian Steppe: the 2008 DUVEX intensive observational period. SOLA 6:9–12

Shinoda M, Gillies JA, Mikami M, Shao Y (2011) Temperate grasslands as a dust source: knowledge, uncertainties, and challenges. Aeolian Res 3:271–293

Sterk G, Raats PAC (1996) Comparison of models describing the vertical distribution of wind eroded sediment. Soil Sci Soc Am J 60:1914–1919

Sterk G, Stein A, Stroosnijder L (2004) Wind effects on spatial variability in pearl millet yields in the Sahel. Soil Tillage Res 76:25–37

Tanaka TY, Chiba MA (2006) A numerical study of contributions of dust source regions to the global dust budget. Glob Planet Chang 52:88–104

Tegen I, Harrison SP, Kohfeld KE, Engelstaedter S, Werner M (2002) Emission of soil dust aerosol: anthropogenic contribution and future changes. Geochim Cosmochim Acta 66:A766

Tsoar H, Pye K (1987) Dust transport and the question of loess formation. Sedimentology 34:139–153

Wen HY, Niu DC, Fu H, Kang J (2013) Experimental investigation on soil carbon, nitrogen, and their components under grazing and livestock exclusion in steppe and dessert grassland, Northwestern China. Environ Earth Sci 70:3131–3141

WRB (2006) World reference base for soil resources. World Soil Research Reports 103. FAO, Rome

Zender CS, Miller RL, Tegen I (2004) Quantifying mineral dust mass budgets: terminology, constraints, and current estimates. EOS Trans 85:509–512

Zhang Z, Wieland R, Reiche M, Funk R, Hoffmann C, Li Y, Sommer M (2012) Identifying sensitive areas of wind erosion in the Xilingele grassland by computational fluid dynamics modelling. Ecol Infor 8:37–47

Zhao TL, Gang SL, Zhang XY, Blanchet JP, McKendry IG, Zhou ZJ (2006) A simulated climatology of Asia dust aerosol and its trans-Pacific transport. J Clim 19:88–103

Zobeck TM, Sterk G, Funk R, Rajot JL, Stout JE, Van Pelt RS (2003) Measurement and data analysis methods for field scale wind erosion studies and model validation. Earth Surf Process Landf 28:1163–1188